REGULAR PAPER

Laser self-mixing interferometry for micro-vibration measurement based on inverse Hilbert transform

Zihua Zhang[1] · Luqing Sun[2] · Chengwei Li[1] · Zhen Huang[3]

Abstract
A novel micro-vibration reconstruction method based on inverse Hilbert transform is presented. By inversing either side of the SMI signal after Hilbert transform, micro-vibration can be reconstructed quickly and conveniently. In the paper, the principle of inverse Hilbert transform algorithm is studied. And, the effectiveness of the method is verified through simulated signals, and several experiments are carried out, including the self-mixing signal affected by speckle effect. The experimental results show that the external cavity phase can be rapidly extracted by inverse Hilbert transform algorithm, and the relative error is no more than 7%.

1 Introduction

As the high precision manufacturing technology advances, self-mixing interferometry (SMI) has attracted much attention because of its inherent simplicity, compactness and self-aligning [1–3]. It has been widely used in displacement and vibration measurement field [4–6]. Semiconductor laser self-mixing interference (SMI) is an interference phenomenon, which is caused by the reflection or scattering of some light back into the laser cavity and mixed with the light in the internal cavity. Feedback light carries the vibration information, which can adjust the laser diode (LD) output power and optical wavelength, this phenomenon is called SMI.

The micro-vibration was measured by counting the peak value of interference signal using SMI method. However, by counting peaks we can only get $\lambda/2$ resolution, to increase the resolution, a lot of methods have been proposed, in which the injection current modulation is one of the phase measurement methods [5, 7], and some demodulation methods have been reported, but the current modulation method can change the wavelength of laser diode and it also needs extra modulation equipment. Bes et al. presented an auto-adaptive signal handing algorithm which can value the light feedback level parameter C [8], the proposed reconstruction algorithm can achieve a maximum reconstructed accuracy of 40 nm with the moderate feedback parameter. Guo used an electro-optic modulator (EOM) in an external cavity and developed a sinusoidal phase modulating technique [5], and it can effectively improve the resolution of vibration measurement to a few nanometers. Guo presented an orthogonal demodulation method [9], and used EOM to obtain the modulation phase, which can only be used in the case of weak feedback. In 2013, Wang et al. improved fringe precision to near $\lambda/4$ and $\lambda/6$ of the object vibration by employing an external reflecting mirror [10], however, the angle between the external reflecting mirror and vibration object must be adjusted carefully. Arriaga et al. proposed a robust phase calculation approach to detect self-mixing signals from rough surface targets based on Hilbert transform [11], which can ignore the dynamic variations in the feedback level even face to speckle degradations. However, using the proposed phase extraction method to find an appropriate threshold is a bit complicated. Tao et al. proposed a signal-processing method to obtain a couple of exact quadrature signals based on Hilbert transform to extract vibration [12]. But, the combination of the

✉ Zihua Zhang
  zhanghua_0813@126.com

✉ Chengwei Li
  lcw@hit.edu.cn

[1] School of Instrumentation Science and Engineering, Harbin Institute of Technology, Harbin 150001, China

[2] School of Electrical Engineering, Wuhan University, Wuhan 430072, China

[3] School of Physics Science and Technology, Lingnan Normal University, Zhanjiang 524048, China

continuous wavelet transform (CWT) algorithm makes the vibration reconstruction algorithm complex. In 2019, our team proposed a demodulation algorithm based on multiple Hilbert transform to extract vibration [13]. However, the algorithm of multiple Hilbert transformation has no reasonable mathematical model analysis at that time.

In the study, we proposed a novel self-mixing interferometry phase extraction method based on inverse Hilbert transform algorithm. First, Hilbert transform (HT) is applied to the self-mixing signal. However, combing Doppler effect [12], the HT of SMI signal equals a phase shift of $-\pi/2$ relative to original signal when the external object moves towards the semiconductor laser [14], otherwise a phase shift of $+\pi/2$ to original signal when the external object runs away. Second, to extract the external phase correctly, we inverse the Hilbert transform of the right-inclined SMI signal to make phase compensation. Further, a same phase shift of $-\pi/2$ compared with original SMI signal on both sides of the reverse point was obtained, the algorithm is named inverse Hilbert transform (IHT).

In this paper, the theory of SMI phenomenon is analyzed by two Fabry–Perot cavities and IHT method is analyzed theoretically and deduced mathematically. The major advantage of the method is that it does not involve any complicated calculation and removes the need for optical/electro-mechanical component, which can further ignore the dynamic variations in the feedback level even face to speckle degradations. At last, the validity of the method is verified by simulations and experiments. The proposed method increases the resolution well beyond half-fringe.

2 Theory of self-mixing interferometry

When the distance between the measurement object and LD is less than half of the laser coherent length, the basic theories of the self-mixing interference phenomenon can be explained by two Fabry–Perot cavities as shown in Fig. 1 [9], in which r_1 and r_2 are the amplitude reflectivity of laser diode facets, r_3 is the amplitude reflectivity of the external target, l denotes the length of the internal cavity and L is the length of the external cavity. And the output
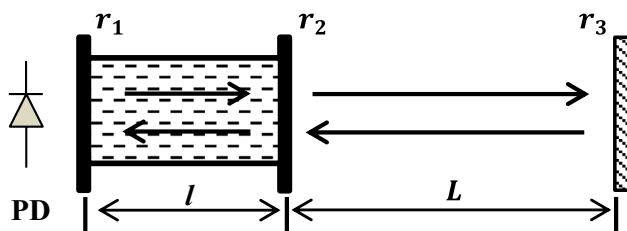

Fig. 1 Schematic diagram of self-mixing interference

SMI signal is monitored by a photodiode (PD), which is encapsulated in LD.

When part of the laser beam is scattered into the internal cavity by the measurement object, self-mixing interference happens. And according to [3, 14], the rear PD outputs in semiconductor laser diodes had the features that SMI edges tilt to the right when the external target is far away from LD, and to the left when the target is running close to LD. Neglecting the multiple reflections in the external cavity, the SMI phase and LD's output power equation can be presented respectively:

$$\omega_0 \frac{2L(t)}{c} = \omega_F \frac{2L(t)}{c} + C\sin\left[\omega_F \frac{2L(t)}{c} + \arctan\alpha\right], \quad (1)$$

$$P_F = P_0[1 + m\cos(\phi_F(t))], \quad (2)$$

where ω_0 and P_0 are the angular frequency and the laser output power without optical feedback, respectively, ω_F and P_F are the angular frequency and the output power with optical feedback, respectively. c is the speed of light in a vacuum. And α is the line-width enhancement parameter, m is the modulation coefficient of self-mixing [15, 16]. The feedback level factor is presented as C, which can be written as:

$$C = \frac{\tau_L}{\tau_l} \zeta \sqrt{1 + \alpha^2}, \quad (3)$$

where τ_L and τ_l denote the round-trip time within the external cavity and internal laser cavity, which can be written as $\tau_L = 2L/c$ and $\tau_l = 2l/c$ respectively. The parameter ζ is the coupling coefficient. And based on Ref. [17], self-mixing interference fringes are categorized into three regions: (a) a weak feedback level $0 < C < 1$, (b) $1 \leq C \leq 4.6$ a moderate feedback level, and (c) $C > 4.6$ a strong feedback level. As C value increases, it will suffer from hysteresis and fringe loss [18]. Therefore, in this paper, only weak and moderate feedback regimes are discussed.

Equation (1) can be simplified by $\phi_0(t) = \omega_0 \times 2L(t)/c$ and $\phi_F(t) = \omega_F \times 2L(t)/c$.

$$\phi_0(t) = \phi_F(t) + C\sin[\phi_F(t) + \arctan\alpha], \quad (4)$$

in the equation, ϕ_F and ϕ_0 are the external round-trip phase with and without light feedback, respectively. After that, $\phi_0(t) = \omega_0 \times 2L(t)/c$ can be expressed as:

$$L(t) = \phi_0(t)\frac{c}{2\omega_0} = \frac{\lambda_0}{2 \times 2\pi}\phi_0(t), \quad (5)$$

where λ_0 represents the initial wavelength of the laser. Given the weak feedback regime [10, 19], $\phi_0(t) \approx \phi_F(t)$, Eq. (5) can be expressed as follows:

$$L(t) = \frac{\lambda_0}{2 \times 2\pi} \phi_F(t). \tag{6}$$

3 Theory of inverse hilbert transform

To extract the external phase $\phi_F(t)$ and reconstruct the micro-vibration correctly, a novel method on account of Hilbert transform (HT) is presented. Following equation is the Hilbert transformation:

$$H[\cos(\phi_F(t))] = \frac{1}{\pi} \int_{-\infty}^{+\infty} \frac{\cos(\phi_F(t))}{t - \tau} d\tau. \tag{7}$$

Equation (7) represents HT as a convolution calculation of external phase $\phi_F(t)$ with an impulse response function $h(t) = 1/\pi t$, and the frequency response of the impulse response function takes below form according to Ref. [12]

$$H(\omega) = \begin{cases} -j, & \omega > 0 \\ +j, & \omega < 0 \end{cases}, \tag{8}$$

where ω is the angular frequency of the original SMI signal, Eq. (8) implies that the HT of SMI signal equals a phase shift of $-\pi/2$ relative to original signal when $\omega > 0$, otherwise a phase shift of $+\pi/2$ to original signal when $\omega < 0$.

According to the Doppler effect, as the external object moves towards the semiconductor laser, the frequency shift is positive ($\omega > 0$) and the edges of SMI tilt to the left. As the external object runs away, the frequency shift is negative ($\omega < 0$) and the edges of SMI tilt to the right. Now with the combination of Eq. (8), the left-inclined fringes of SMI obtain a phase shift of $-\pi/2$ through Hilbert transform of self-mixing signal, which can be written as $\cos(\phi_F(t) - \pi/2) = \sin(\phi_F(t))$. And the right-inclined fringes of SMI obtain a phase shift of $+\pi/2$ through Hilbert transform of self-mixing signal, which can be written as $\cos(\phi_F(t) + \pi/2) = -\sin(\phi_F(t))$. Figure 2a illustrates the simulation of self-mixing signal, Ref. [3] gives the reverse point R between these two inclined fringes. The Hilbert transform of self-mixing signal is shown in Fig. 2b.

As to extract the external phase correctly, we inverse either side of the HT of SMI signal, which is original right-inclined fringes of self-mixing signal or the original left-inclined fringes of self-mixing signal. The purpose is to make a phase compensation for the HT of SMI signal, so as to ensure the same phase shift of the original SMI signal on both sides of the reverse point.

Based on the above analysis, this paper proposes an algorithm to inverse the Hilbert transform of the right-inclined SMI signal, the algorithm is named inverse
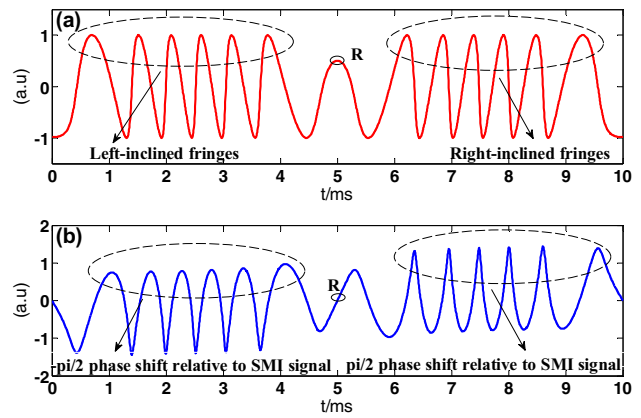

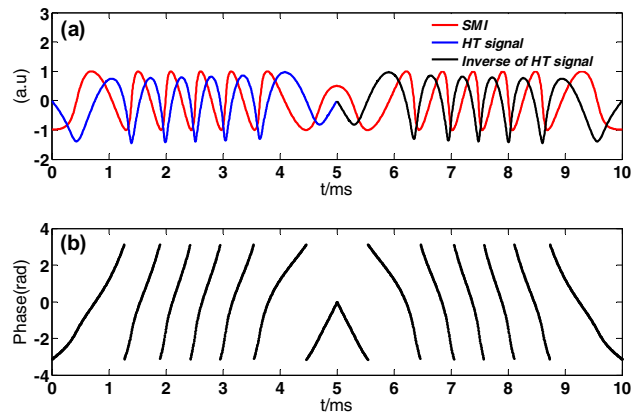Fig. 2 Hilbert transform of self-mixing signal. a Simulation of SMI: $C = 0.5$, b Hilbert transform signal

Fig. 3 Transform algorithm. a Self-mixing and IHT signal in comparison, the red curve is SMI signal, the blue one is HT signal and the black is the inverse of HT signal, b wrapped phase

Hilbert transform (IHT). And then we can get a same phase shift of $-\pi/2$ compared with original SMI signal on both sides of the reverse point, then, it can be represented as $\sin(\phi_F(t))$. Figure 3 shows the transform simulation process. In Fig. 3a, the comparison of the self-mixing signal and IHT signal is presented, of which the blue curve is Hilbert transform signal and the black one is the inverse of HT signal. Figure 3b shows the wrapped phase.

Figure 4 shows the flow chart of IHT algorithm. First, we filter and normalize the SMI signal, and then we perform Hilbert transform of SMI signal, decide vibration inverse point of external object, and inverse the Hilbert transform signal of the right-inclined self-mixing signal. After that, the combination with the HT of left-inclined SMI signal on the reverse point forms $\sin(\phi_F(t))$. At last, $\tan\phi_F(t)$ is acquired using the combination IHT signal dividing by self-mixing interference signal.
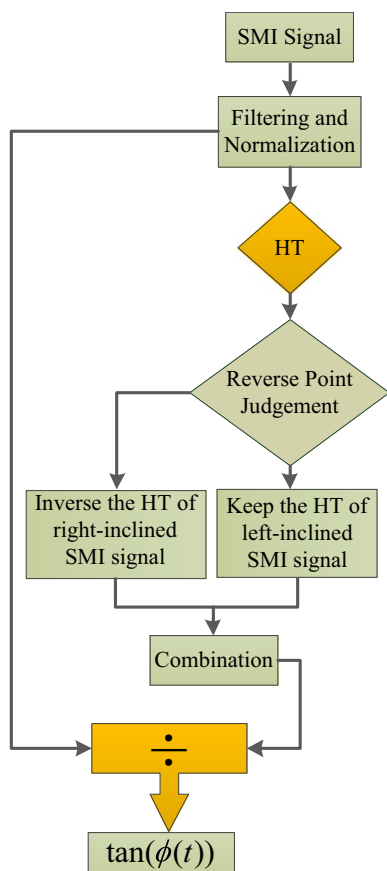
Fig. 4 Flow chart of IHT method

The phase $\phi_{\mathrm{F}}(t)$ wrapped within the region of $-\pi$ and $+\pi$ is obtained. With a phase extraction course, the external object vibration can be reconstructed based on Eq. (6).

4 Matlab simulation

4.1 The simulation of harmonic vibration

The measurement of micro-vibration using the proposed method has been tested on MATLAB. First, the numerical simulation has been operated with weak feedback level $C = 0.2$, and line-width enhancement parameter is chosen as 4.6. As shown in Fig. 5a, the harmonic vibration is driven with a frequency of 10 Hz and an amplitude of 2.6 μm ($A = 4\lambda_0$). And the original wavelength is 650 nm without optical feedback, the original external cavity length between laser and external object is $L_0 = 0.1$ m. The sampling points of the simulation are 5000 under sampling frequency of 50 kHz. The red curve is self-mixing interference fringes and the blue one presents IHT signal, it has a same phase shift of $-\pi/2$ compared with the original self-mixing signal as presented in Fig. 5b. Figure 5c shows the reconstructed
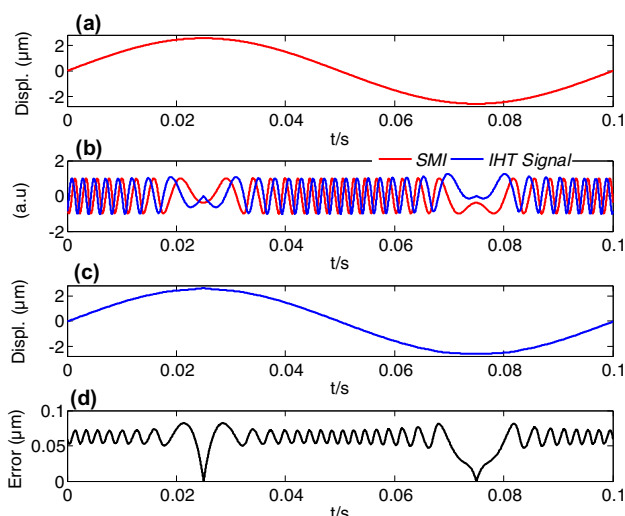

Fig. 5 Simulation with $C = 0.2$. **a** Harmonic vibration, **b** the red curve presents the SMI signal and IHT curve is presented in blue, **c** reconstructed vibration, **d** error

vibration and Fig. 5d shows the absolute error between the reference and the reconstructed vibration.

Figure 6 presents simulation results with an amplitude of 2.3 μm and feedback parameter $C = 2.5$ with moderate feedback level. The sampling points of the simulation are 10000 under sampling frequency of 50 kHz. Besides, other parameters are the same with Fig. 5. Figure 6a presents a simulated harmonic vibration with a frequency of 5 Hz. Figure 6b shows the SMI signal. The reconstructed vibration is shown in Fig. 6c. Figure 6d presents the reconstructed absolute error.
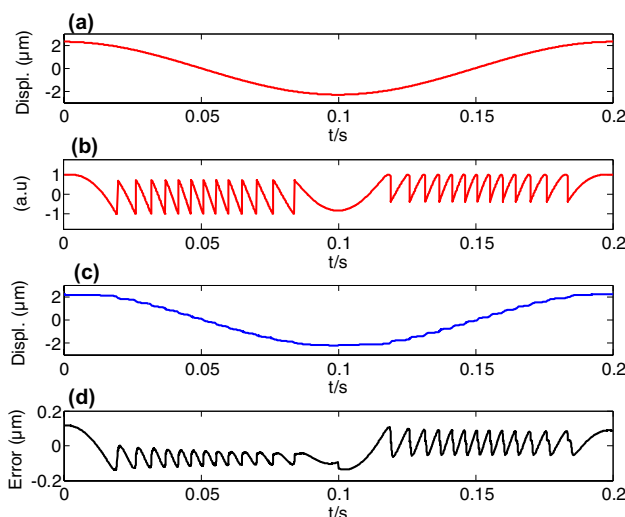

Fig. 6 Simulation with $C = 2.5$. **a** Harmonic vibration, **b** SMI signal, **c** reconstructed vibration, **d** the reconstructed absolute error

The MATLAB simulation results show that the maximum absolute error is $\sim \lambda_0/7.9$ (82 nm), when the peak-to-peak amplitude is 5.2 µm of the simulated harmonic vibration with $C = 0.2$. And the maximum absolute error is $\sim \lambda_0/4.7$ (137 nm), when the peak-to-peak amplitude is 4.6 µm of the simulated harmonic vibration with $C = 2.5$. The algorithm proposed in this paper can be well applied to the field of micro-vibration displacement measurement under weak feedback regime, and the maximum reconstructed error occurs at the reverse point of the vibrating object.

4.2 Speckle disturbance vibration reconstruction simulation

As the laser spot has finite size, SMI signal in this condition exhibits an envelope shape in time domain due to the variation which results of the incoherent superposition of different waveforms reflected by rough targets, and it is called speckle effect [11]. In order to simulate the phenomenon, we plot Fig. 7 with amplitude attenuation. So under this condition, the adaptive threshold algorithm [20] is not useful here. Since each fringe contributes to half LD's wavelength of target vibration, reconstruction of a target vibration from SMI signal relies on the proper extraction of external phase. The proposed IHT algorithm in this paper can well adapt to the amplitude attenuation of SMI signal caused by speckle effect.

The simulation has been operated under weak feedback regime with $C = 0.1$, and line-width enhancement parameter is chosen as 4.6. As shown in Fig. 8a, the red curve represents self-mixing signal with attenuation of harmonic vibration which is driven with a frequency of 10 Hz and an amplitude of 3.2 µm, the black curve is the IHT signal. And

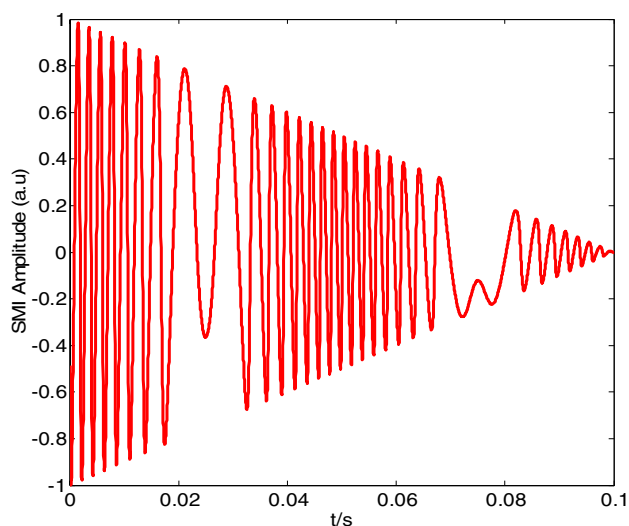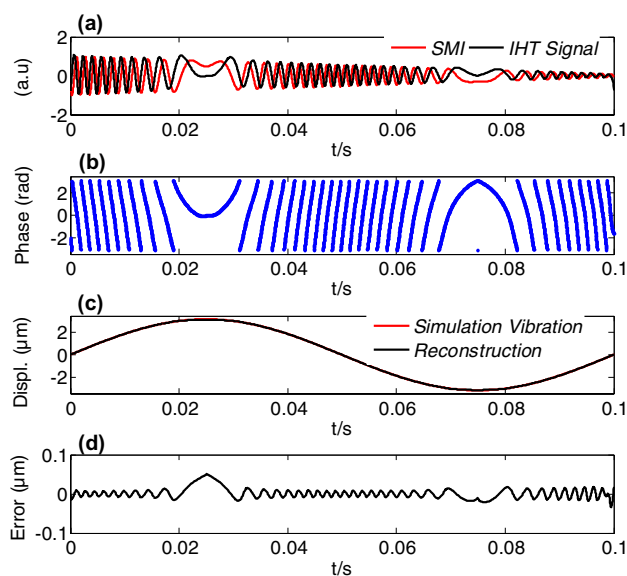**Fig. 8** Reconstruction simulation. **a** The red curve represents SMI signal with amplitude attenuation, the black curve is the IHT signal, **b** wrapped phase, **c** displacement of the reference (red) and the reconstruction (black), **d** error

$\lambda_0 = 650\,nm$, the original external cavity length between LD and the object is $L_0 = 0.1$ m. Figure 8b presents the wrapped phase $\arctan 2[\phi_F(t)]$. In Fig. 8c, the red curve is the simulated sinusoidal motion of external object, and the black curve is the reconstructed vibration. And the reconstructed error is presented in Fig. 8d, in which we can get the maximum error is $\sim \lambda_0/12.7$ (51 nm).

The simulation results show that the micro-vibration reconstructed method for laser self-mixing interferometry based on inverse Hilbert transform can properly extract external phase with weak or moderate optical feedback level, and it can also well adapt to the amplitude attenuation variation of SMI signal caused by speckle effect.

5 Experimental setup and results

The proposed method has been tested experimentally. The schematic diagram of the experimental setup is shown in Fig. 9. It includes a semiconductor laser diode (QL65D5SA, QSI, 650 nm) packaged with a photo-diode (PD), and its power is 5 mW, which is driven by a constant current driver (LD1255R, Thorlabs). A piezoelectric transducer (PZT, P753.1CD, PI) with a travel of 12 µm is selected to be used as a vibrating object, which is a high-precision reference with a resolution of 0.05 nm when performing vibration measurement tests. To perform experiments with the proper feedback regime, a variable attenuator (VA) is used to control the amount of reflected beam into the internal cavity. The PD detects the current change of the laser output power,
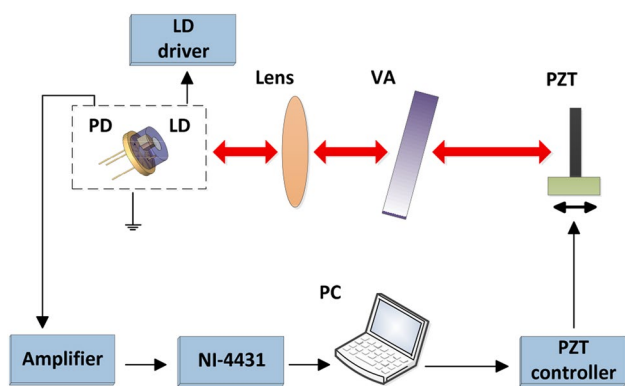
Fig. 7 Simulation of the amplitude attenuation of SMI signal

Fig. 9 Schematic diagram of the experimental setup

and the current signal is converted into voltage by the transconductance amplifier. We use a PC to process the data, which is obtained through data acquisition card (NI-4431).

5.1 PZT harmonic vibration measurement

Figure 10 shows the measurement process that the tests are operated with weak feedback level. The external object vibrates a sinusoidal movement, which has a frequency of 5 Hz and a peak-to-peak amplitude of 4 μm. The experimental sampling frequency is 50 kHz and 20000 points in total. In the experiment, a 500 Hz low-pass filter is used to filter the PD output acquisition signal, and then the filtering signal is normalized. The red curve in Fig. 10a is self-mixing signal with weak feedback level for $C = 0.1$, and IHT signal

is the black curve. Figure 10b presents the wrapped phase $\phi_F(t)$. And in Fig. 10c, the movement of reference object is shown in red and the reconstructed harmonic movement is shown in black. The object movement reconstructed error is shown in Fig. 10d.

Then, the proposed algorithm has been operated with moderate feedback regime as shown in Fig. 11. The experimental parameters are the same with Fig. 10, except the feedback parameter which is estimated using the algorithm provided in ref. [8] is 2.5. With moderate feedback regime, Eq. (5) is used to carry out vibrated reconstruction. The red curve in Fig. 11a shows the experimental self-mixing signal with $C = 2.5$, and the black curve is IHT signal. Figure 11b presents the wrapped phase $\phi_F(t)$. And Fig. 11c shows the reference object movement in red and the reconstructed movement in black. And the object movement reconstructed absolute error is shown in Fig. 11d.

Experimental results show that the maximum absolute error is $\sim \lambda_0/6.2$ (105 nm), when the peak-to-peak amplitude is 4.0 μm of the object harmonic vibration with $C = 0.1$. And the maximum error is about $\lambda_0/4.16$ (156 nm), when the peak-to-peak amplitude is 4.0 μm of the object harmonic vibration with $C = 2.5$.

Several group of repeated tests with feedback parameter $C = 0.1$ have been done to illustrate the reliability. And the external object moves a harmonic vibration with a frequency of 5 Hz and a peak-to-peak amplitude from 1 to 10 μm, with a step length of 1.0 μm. Ten times experiments were repeated in each group of tests. Figure 12 shows the analysis
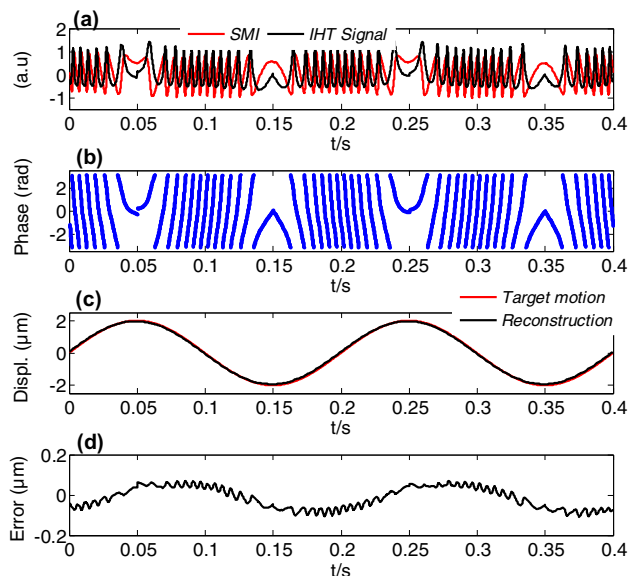

Fig. 10 Object movement. **a** Signal of the experimental SMI in red and the IHT signal in black, **b** wrapped phase, **c** displacement of the reference (red) and the reconstruction (black), **d** error
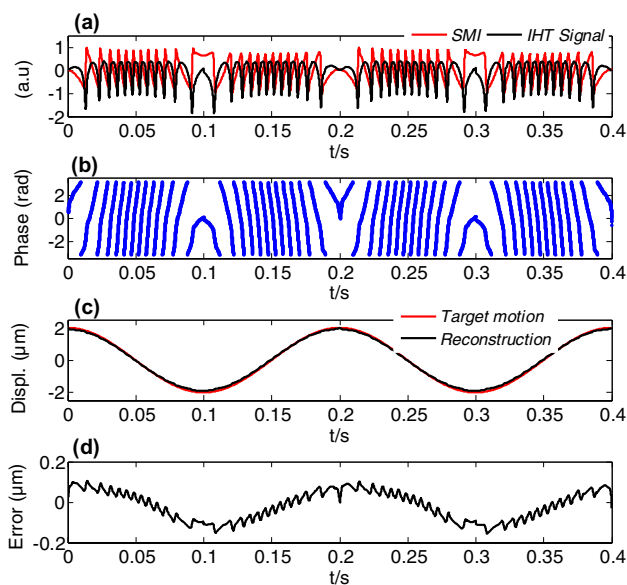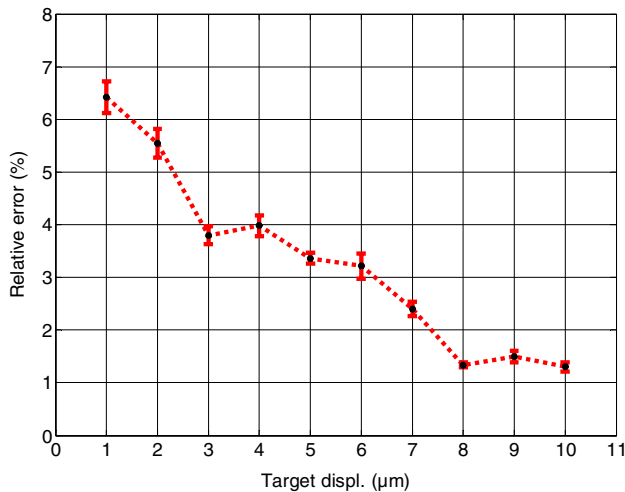

Fig. 11 Object movement with $C = 2.5$. **a** Signal with the experimental SMI in red and the IHT signal in black, **b** wrapped phase, **c** displacement of the reference (red) and the vibration reconstruction (black), **d** error

Fig. 12 Measurement error

Fig. 13 Experimental of SMI affected by speckle effect. **a** SMI signal disturbed by speckle, **b** wrapped phase, **c** target motion (red) and reconstructed displacement (black), **d** error

results, of which the black points are relative error of measurement movement with weak feedback level, the red error bars are the standard error.

It can be seen from Fig. 12 that the mean relative error of the vibrated reconstruction tests are less than 7%. With the increasing of harmonic amplitude, error of vibrated reconstruction tends to decrease gradually.
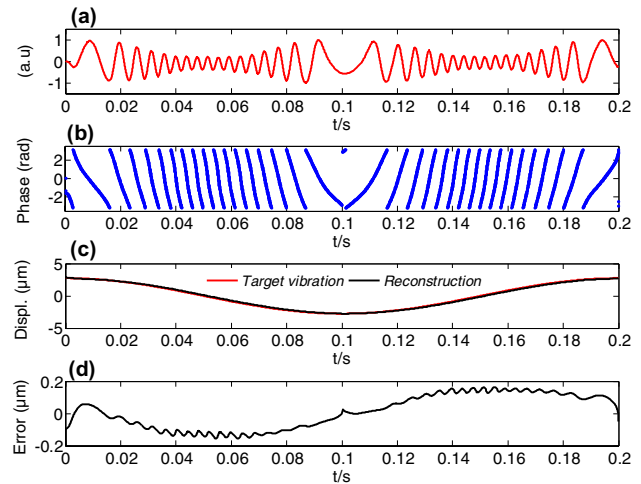
5.2 Speckle effect of SMI experiments

Due to the influence of surface roughness of the measured object in the experiment, the SMI signal is often accompanied by speckle effect. In this experiment, we put a piece of white paper on the surface of the vibrated object to simulate the rough surface. And the PZT is controlled to move at a sinusoidal form with a frequency 5 Hz, a peak-to-peak amplitude 5.5 μm. The sampling rate of the A/D card is 50 kHz. The test results are shown in Fig. 13. In Fig. 13a, the curve represents self-mixing signal of the harmonic vibration, whose amplitude is influenced by speckle effect. Following phase unwrapping steps, the real phase is regained as $arctan2[\phi_F(t)]$ in Fig. 13b. And Fig. 13c, the red curve is the object's sinusoidal vibration and the black curve is the reconstructed vibration. The reconstructed absolute error is presented as Fig. 13d, in which we can get a maximum error 164 nm.

From Fig. 13, it can be seen that the algorithm can reconstruct micro-vibration effectively when the self-mixing signal is disturbed by speckle effect.

5.3 Aleatory vibration measurement

Finally, to verify the generality of the proposed algorithm, a group of aleatory vibration reconstruction experiments

has been performed. The object movement is a sinusoidal form of 10 Hz modulated by a 5 Hz form with a modulated depth of 50%, which is shown in Fig. 14c in red, and the black curve is the reconstructed vibration. The curve in Fig. 14a shows the experimental self-mixing signal of the external object. And Fig. 14b presents the wrapped phase. The reconstructed error is shown in Fig. 14d and the measurement error is ~ 0.114 μm for a maximum sinusoidal amplitude 6.0 μm, which shows a good performance of the algorithm proposed in this paper.
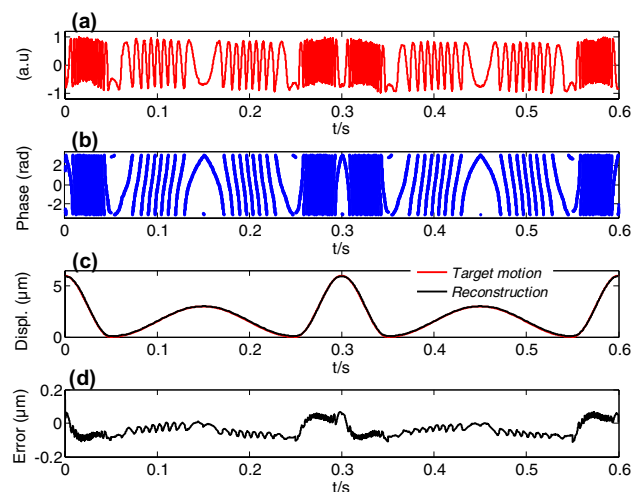
Fig. 14 Aleatory movement. **a** Self-mixing signal of aleatory movement, **b** wrapped phase, **c** displacement of the reference (red) and the reconstruction (black), **d** error

6 Conclusion

An effective micro-vibration analysis method is presented in this article. By inversing the Hilbert transform of the right-inclined self-mixing signal, we get a same phase shift of $-\pi/2$ on both sides of the reverse point, and the micro-vibration can be measured with weak or even moderate feedback regime. The repeated experimental results show that the error is less than 7%. Then, the reconstructed ability of the method is verified when the measured object is affected by speckle effect. The optical path is simple and does not need complicated calculation and it can be applied to the vibration measurement field using semiconductor laser self-mixing interference technique.

Compliance with ethical standards

Conflict of interest The authors declare that there is no conflict of interests regarding the publication of this paper.

References

1. Taimre, T., Nikolić, M., Bertling, K., Lim, Y.L., Bosch, T., Rakić, A.D.: Laser feedback interferometry: a tutorial on the self-mixing effect for coherent sensing. Adv. Opt. Photonics **7**, 570 (2015)
2. Donati, S.: Developing self-mixing interferometry for instrumentation and measurements. Laser Photonics Rev. **6**, 393–417 (2012)
3. Fan, Y., Yu, Y., Xi, J., Chicharo, J.F.: Improving the measurement performance for a self-mixing interferometry-based displacement sensing system. Appl. Opt. **50**, 5064–5072 (2011)
4. Jiang, C., Zhang, Z., Li, C.: Vibration measurement based on multiple self-mixing interferometry. Opt. Commun. **367**, 227–233 (2016)
5. Guo, D.M., Wang, M.: Self-mixing interferometry based on a double-modulation technique for absolute distance measurement. Appl. Opt. **46**, 1486–1491 (2007)
6. Jiang, C., Wen, X., Yin, S., Liu, Y.: Multiple self-mixing interference based on phase modulation and demodulation for vibration measurement. Appl. Opt. **56**, 1006 (2017)
7. Suzuki, T., Hirabayashi, S., Sasaki, O., Maruyama, T.: Self-mixing type of phase-locked laser diode interferometer. Opt. Eng. **38**, 543–548 (1997)
8. Bes, C., Plantier, G., Bosch, T.: Displacement measurements using a self-mixing laser diode under moderate feedback. IEEE Trans. Instrum. Meas. **55**, 1101–1105 (2006)
9. Guo, D.: Quadrature demodulation technique for self-mixing interferometry displacement sensor. Opt. Commun. **284**, 5766–5769 (2011)
10. Wang, L., Luo, X., Wang, X., Huang, W.: Obtaining high fringe precision in self-mixing interference using a simple external reflecting mirror. IEEE Photonics J. **5**, 6500207 (2013)
11. Arriaga, A.L., Bony, F., Bosch, T.: Speckle-insensitive fringe detection method based on Hilbert transform for self-mixing interferometry. Appl. Opt. **53**, 6954–6962 (2014)
12. Tao, Y., Wang, M., Xia, W.: Semiconductor laser self-mixing micro-vibration measuring technology based on Hilbert transform. Opt. Commun. **368**, 12–19 (2016)
13. Zhang, Z.H., Li, C.W., Huang, Z.: Vibration measurement based on multiple Hilbert transform for self-mixing interferometry. Opt. Commun. **436**, 192–196 (2019)
14. Randone, E.M., Donati, S.: Self-mixing interferometer: analysis of the output signals. Opt. Express **14**, 9188 (2006)
15. Donati, S., Giuliani, G.: Analysis of the signal amplitude regimes in injection–detection using laser diodes. In: R.H. Binder, P. Blood, M. Osinski (eds.) Physics and Simulation of Optoelectronic Devices Viii, Pts 1 and 2. SPIE-Int Soc Optical Engineering, Bellingham, pp. 639–644 (2000)
16. Gao, B., Qing, C., Yin, S., Peng, C., Jiang, C.: Measurement of rotation speed based on double-beam self-mixing speckle interference. Opt. Lett. **43**, 1531 (2018)
17. Sacher, J., Elsässer, W., Göbel, E.O.: Intermittency in the coherence collapse of a semiconductor laser with external feedback. Phys. Rev. Lett. **63**, 2224–2227 (1989)
18. Zabit, U., Bony, F., Bosch, T., Rakic, A.D.: A self-mixing displacement sensor with fringe-loss compensation for harmonic vibrations. IEEE Photonics Technol. Lett. **22**, 410–412 (2010)
19. Zhang, Z., Li, C., Huang, Z.: Quadrature demodulation based on lock-in amplifier technique for self-mixing interferometry displacement sensor. Appl. Opt. **58**, 6098–6104 (2019)
20. Huang, Z., Sun, X., Li, C.: Self-mixing interference signal analysis based on Fourier transform method for vibration measurement. Opt. Eng. **52**, 053601 (2013)